WESTERN RESERVE UNIVERSITY

ANNUAL STATUS REPORT

NASA GRANT NsG-655

MARCH 1, 1965-FEBRUARY 28, 1966

CLEVELAND, OHIO

Second Annual Status Report
for the period March 1, 1965 to February 28, 1966
NASA Grant NsG-655/36-013-002
Principal Investigator: Karl J. Casper

Summary

The research covered by this status report is divided into the following topics:

(1) Studies of the response functions of lithium drifted silicon detectors to monoenergetic electrons.

(2) Preliminary investigation of the temperature dependence of the resolution of lithium drifted silicon detectors.

(3) Fabrication of large volume lithium drifted silicon detectors.

(4) Studies of the internal Compton effect using a superconducting magnet beta ray spectrometer.

(5) Ohmic contacts to silicon detectors.

(6) Studies of high Z semiconductors for radiation detectors.

(1) Studies of the response functions of lithium drifted silicon detectors to monoenergetic electrons.

It was proposed to study the response of silicon detectors to electrons of different energies. As reported in the semi-annual status report covering the first six months of this grant year, a beta-ray spectrometer is now under construction. This project has been delayed by late delivery of the electromagnet which, although ordered at the beginning of the grant year, was not received until late in the autumn. Once finished, the spectrometer will be used as a means of obtaining nearly monoenergetic electrons. The continuous beta-ray spectrum of radioisotopes will serve as a source of these electrons. They will be focused on silicon detectors and the response function of the detector will be measured as a function of energy.

At the present time, the spectrometer chamber has been constructed, but a measurement of the magnetic field at various points along the electron path showed that the inhomogeneity of the field would render the experiment impossible. The pole faces are now being reconstructed to provide a more nearly homogeneous field in the chamber. In its most simple form, this amounts to putting annuli on the pole faces in accordance with a calculation by Rose.[1] In our case, the chamber had already been constructed and fit rather closely between the faces. Necessarily, the pole faces are being reconstructed and are also being made more nearly parallel than the ones originally supplied by the magnet manufacturer.

The measurement of the magnetic field shows that it will be possible to focus electrons up to 4 MeV with a power supply already available. The addition of the Rose ring pole faces will reduce the field slightly, but it should still be possible to focus electrons greater than 3 MeV which means that the energy range of greatest importance will be covered. Operation of the spectrometer is anticipated to take place this summer.

(2) Preliminary investigation of the temperature dependence of the resolution of lithium drifted silicon detectors.

Numerous studies have shown that the optimum resolution of a silicon detector is obtained by cooling the detector. In practice, either dry ice (-40°C) or liquid nitrogen (77°K) temperatures are used since these temperatures are the most convenient and inexpensive from the standpoint of availability of coolants. At these low temperatures, the reverse current is reduced thereby minimizing the noise generation in the diode from this current. Cooling below liquid nitrogen temperature provides no improvement since the mobility of the ion pairs decreases below that temperature and the charge collection efficiency is reduced.

Naturally there is considerable interest in optimizing the resolution of silicon detectors. Until recently, this resolution was primarily limited by the electronic preamplifiers available. However, new types of preamplifiers[2] have been developed which contribute less than 1 keV to the overall noise of the system. The problem has therefore reverted back to the resolution of the detector itself.

As part of our investigations into this problem, two pieces of experimental data were considered:

1. Field effect transistors which are essentially bars of silicon do not exhibit their lowest noise characteristic at 77°K, but rather at a slightly higher temperature, between 120°K and 140°K.[3]

2. Some experimental evidence on the resolution of germanium lithium drifted detectors has been obtained by El-Shishini and Zobel.[4] They observed that the resolution of these detectors was not optimized at liquid nitrogen temperatures, but rather at 105°K, although they gave no theoretical explanation of this phenomena.

Both of these results indicated that lithium drifted silicon detectors might also have somewhat better resolution at a temperature above that of liquid nitrogen. A preliminary experiment was carried out to determine if more exact measurements would prove fruitful.

A series of spectra of the internal conversion lines of Bi^{207} were taken with a lithium drifted surface barrier silicon detector at temperatures ranging from liquid nitrogen to room ambient. The resolution of the detector on the 975 keV internal conversion line showed a broad but definite minimum near 160°K. At liquid nitrogen temperature, the resolution is approximately 25% higher than the minimum and at room temperature it is about 400% higher. It should be emphasized that these results are preliminary and were obtained to determine if further

experimentation would prove fruitful. Considerable difficulty was encountered in stabilizing the temperature and measuring it precisely. However, the results are very encouraging and indicate that significant improvement in resolution can be obtained. Further experiments are now in progress and a number of detectors will be examined to determine if a general statement can be made about the optimum operating temperature.

(3) Fabrication of large volume silicon detectors.

A large volume silicon lithium drifted detector has been fabricated and will be tested in April. The detector is a diffused junction device, the drifting being terminated before the entire ingot was drifted.

This detector is shown in Fig. 1. Lithium was diffused into one of the long sides (the top one in the photograph) and drifted to a depth of 1 cm. This left approximately 0.5 cm of p-type material which has been retained in the finished detector since a surface barrier detector would have been somewhat more difficult to handle. The width of the detector is 1.5 cm and the total length is over 12.3 cm. Protons up to 160 MeV in energy can be stopped in a detector of this length.

In preparing such a large detector, some account must be taken of the collection time for the ion pairs produced by an incident particle. The maximum velocity of these pairs is on the order of $3 \times 10^{+7}$ cm/sec at room temperature. This means that for a detector

Fig. 1. Photograph of 18 cm^3 lithium drifted silicon detector in mounting holder.

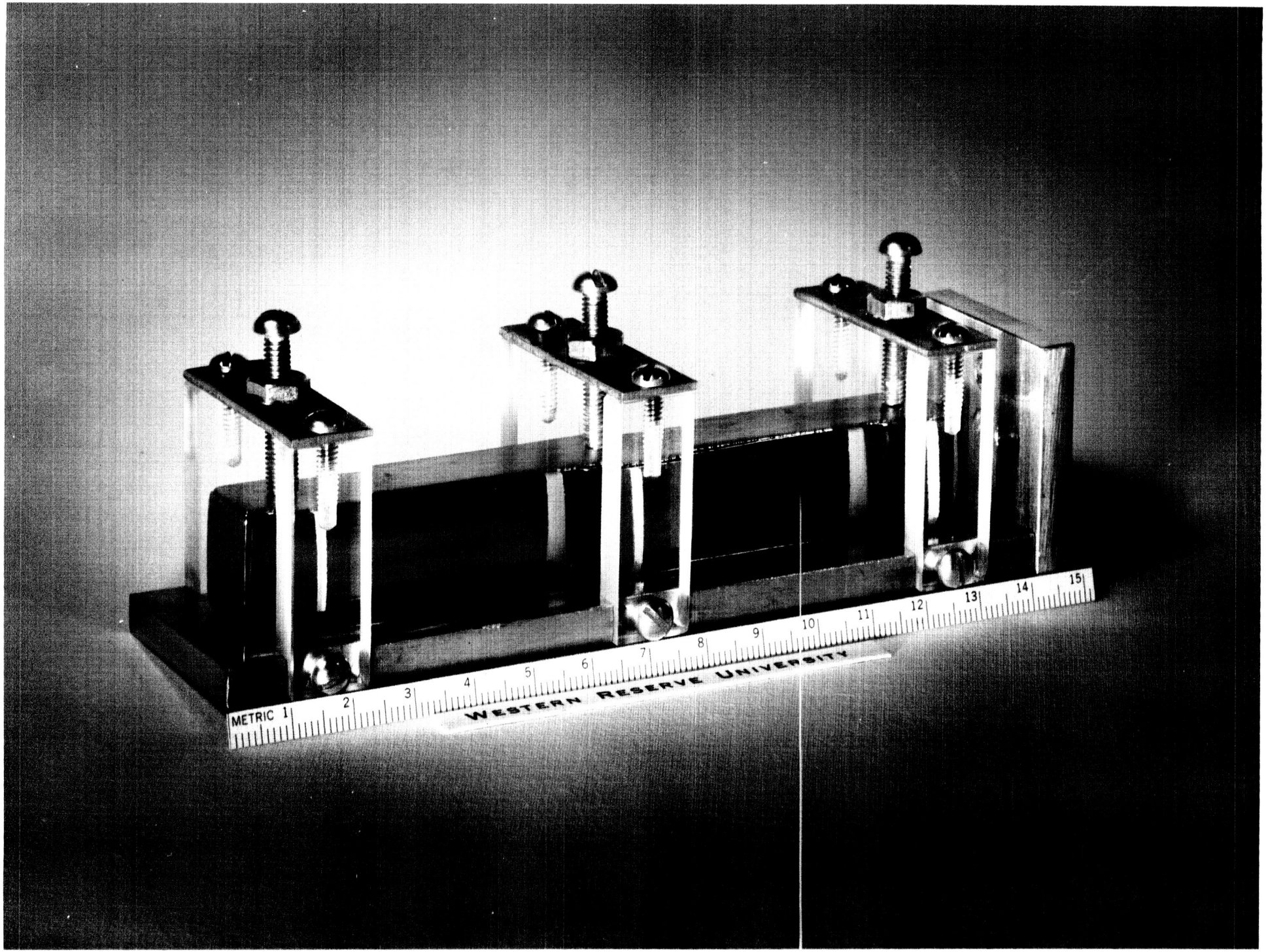
METRIC
WESTERN RESERVE UNIVERSITY

1 cm thick, the collection time may be as long as 300 nanoseconds. For this reason the drift was stopped at 1.0 cm although a somewhat deeper depletion layer could have been drifted. Fortunately, when cooled, the collection times are shortened since the mobility of the ion pairs increases.

Testing of this device will take place sometime in April at the Harvard 160 MeV cyclotron. The detector will be mounted in the special chamber shown in Fig. 2. This chamber has provisions for cooling to liquid nitrogen temperature. A 10 mil beryllium window permits protons to be incident upon the detector with minimal straggling in the window.

(4) Further results in the study of the internal Compton effect measured with a superconducting magnet beta ray spectrometer.

As indicated in the semi-annual status report, the measurement of the internal Compton effect using this spectrometer represents the first direct measurement of the effect. Because of the importance of such an observation and its stimulation of further theoretical effort into the spectral distribution of the electrons and gamma rays resulting from this interaction, it is necessary that the experimental data be as accurate as possible. All possible instrumental effects which might contribute to the spectral distribution must be shown to be negligible and the subsequent paragraphs relate to our efforts along these lines.

A schematic diagram of the superconducting magnet beta-ray spectrometer is shown in Fig. 3. The two lithium drifted silicon surface

Fig. 2. Photograph of large volume silicon detector cryostat.

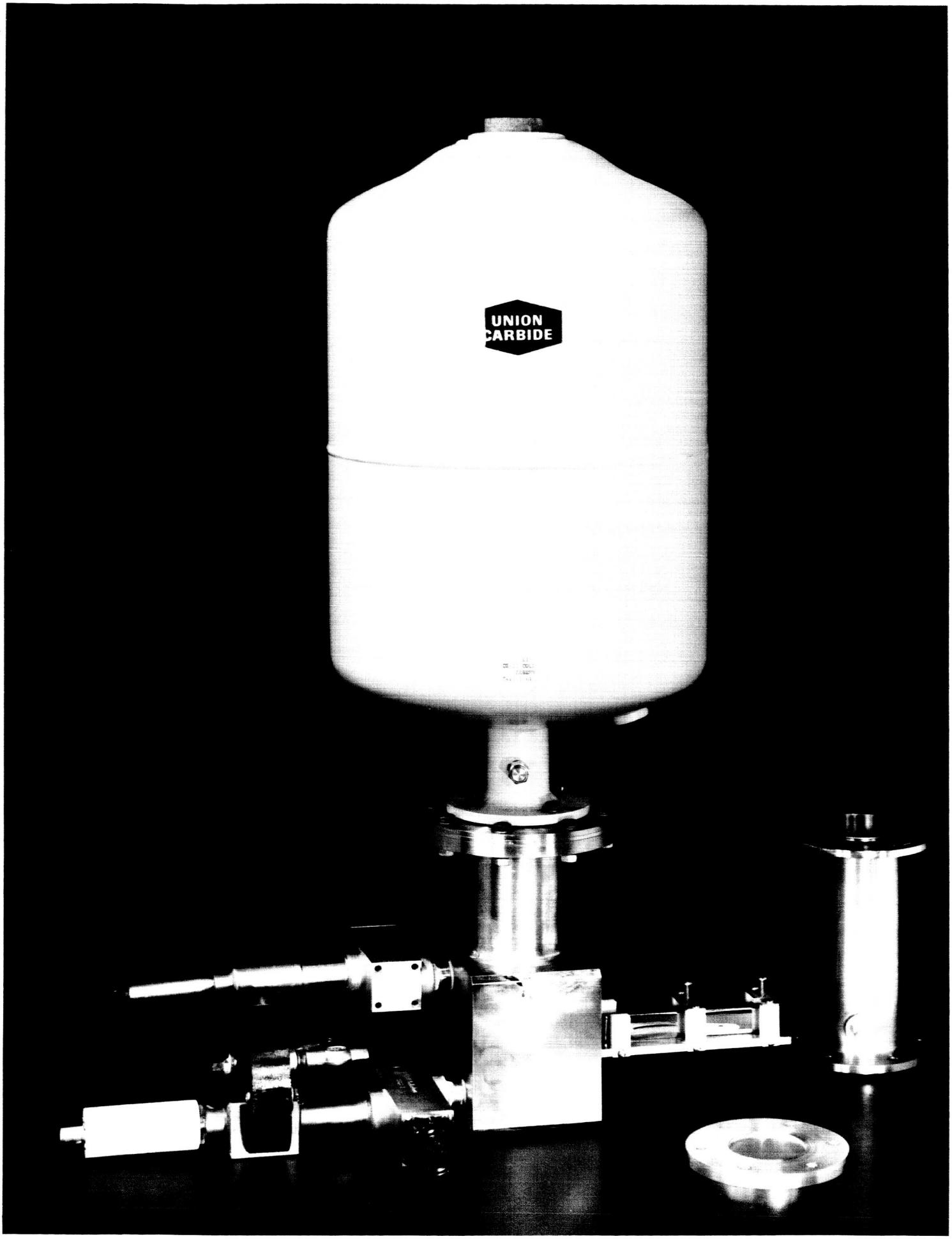
UNION
CARBIDE

Fig. 3. Outline diagram of superconducting magnet beta-ray spectrometer.

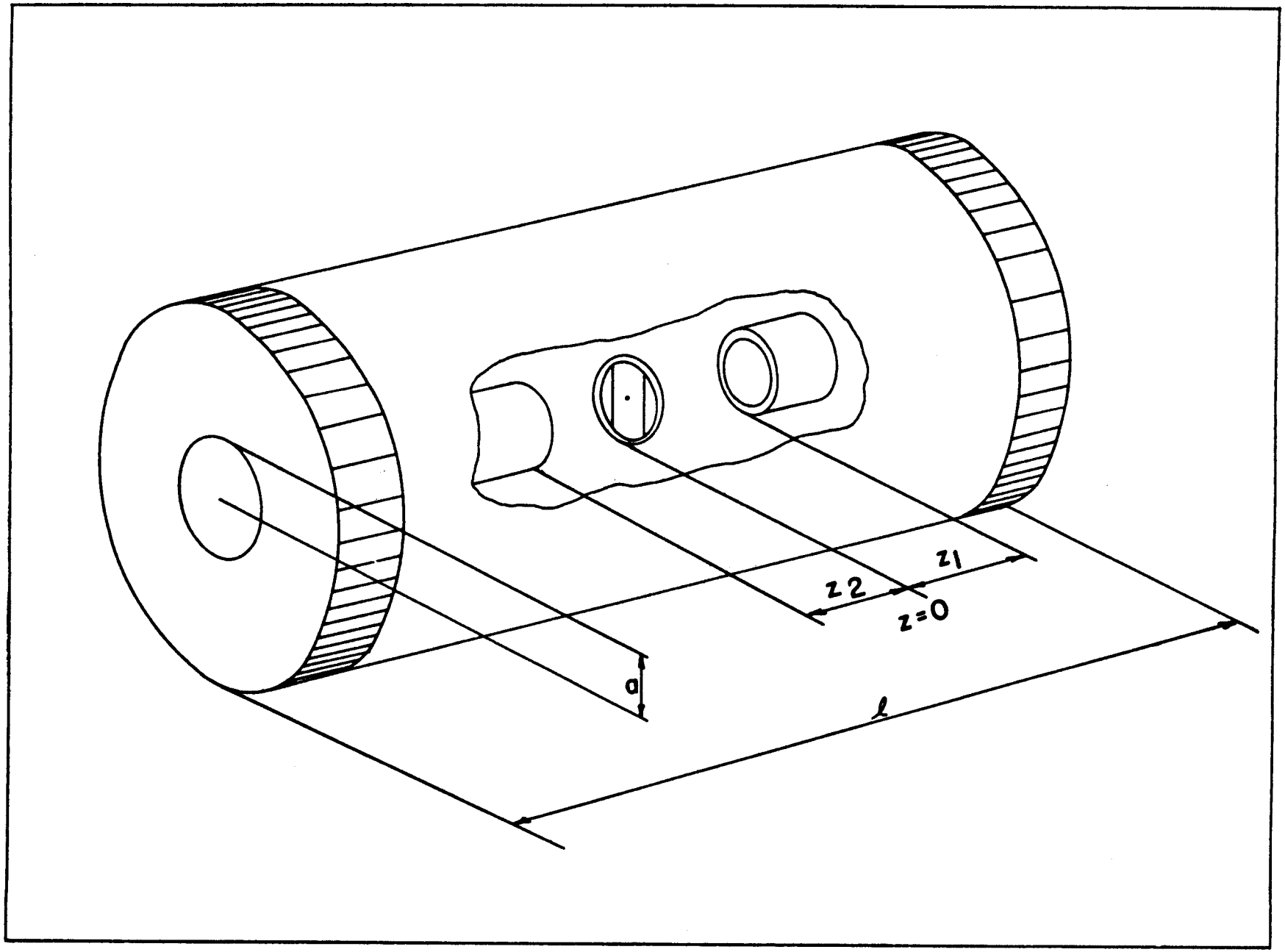
z1
z2
z=0
a
l

barrier detectors were mounted at either end of the solenoid with the radioactive source in the middle. For the measurements of the internal Compton effect, the two detectors were run in parallel which effectively sums the outputs. The output of the preamplifier was fed into a TC200 amplifier and the integration time and differentiation time were set at 0.8 microseconds. The magnetic field along the axis of the spectrometer was set greater than 25 kilogauss for all data runs.

Although it is generally assumed that the field of a solenoid is constant over its working volume, this is the case only if the following two conditions are met:

1) the radius a of the working volume must be much less than the length ℓ of the solenoid;

2) the working volume must be confined to the region well within the area where end effects which distort the field become significant.

For the solenoidal spectrometer used in this experiment, condition (1) is easily met. Referring to Fig. 3, $a = 2.54$ cm, $\ell = 20.3$, and the ratio $\ell/a = 8.0$. Condition (2), however, is not clearly satisfied and a calculation has been done to ensure that at least the minimum field necessary for focusing the electrons is present in the region of the detectors. Referring again to Fig. 3, the positions of the solid state detectors relative to the center of the solenoid are $z_1 = 8.9$ cm and $z_2 = -6.9$ cm. The axial magnetic field of a solenoid, as a function

of the distance along the symmetry axis of the solenoid where this distance is measured from the center, is given by

$$H_z = \frac{I}{2\ell}\left[\frac{(z_i - \frac{\ell}{2})}{[a^2 + (z_i + \frac{\ell}{2})^2]^{\frac{1}{2}}} - \frac{(z_i - \frac{\ell}{2})}{[a^2 + (z_i - \frac{\ell}{2})^2]^{\frac{1}{2}}}\right] \qquad (1)$$

This relation has been numerically evaluated, the field has been normalized to unity at the center of the solenoid, and a graph of the normalized field as a function of distance from the center of the solenoid is shown in Fig. 4. The range of detector positions is shown by the cross-hatched area. In these positions, the field at the detectors is maintained at a value greater than 75% of the maximum available field.

The electrons emitted by the source at the center of the solenoid follow a helical path in the magnetic field. The axis of the helix is displaced from the axis of the solenoid by the radius of the helix. This radius may vary from zero, which corresponds to the electron being emitted directly down the axis of the solenoid, to some radius r_m which corresponds to the electron being emitted normal to the axis of the solenoid. Two problems arise for the latter case:

1) the electrons may have such a large radius of curvature that they may not be incident upon the detector;

2) the component of velocity along the axis of the solenoid may not be large enough that all of the charge will be collected in the integration time of the amplifier. This is of particular concern where the two detectors at either end are run in parallel with their outputs summed and the

Fig. 4. Normalized magnetic field in superconducting solenoid as a function of distance from center of solenoid.

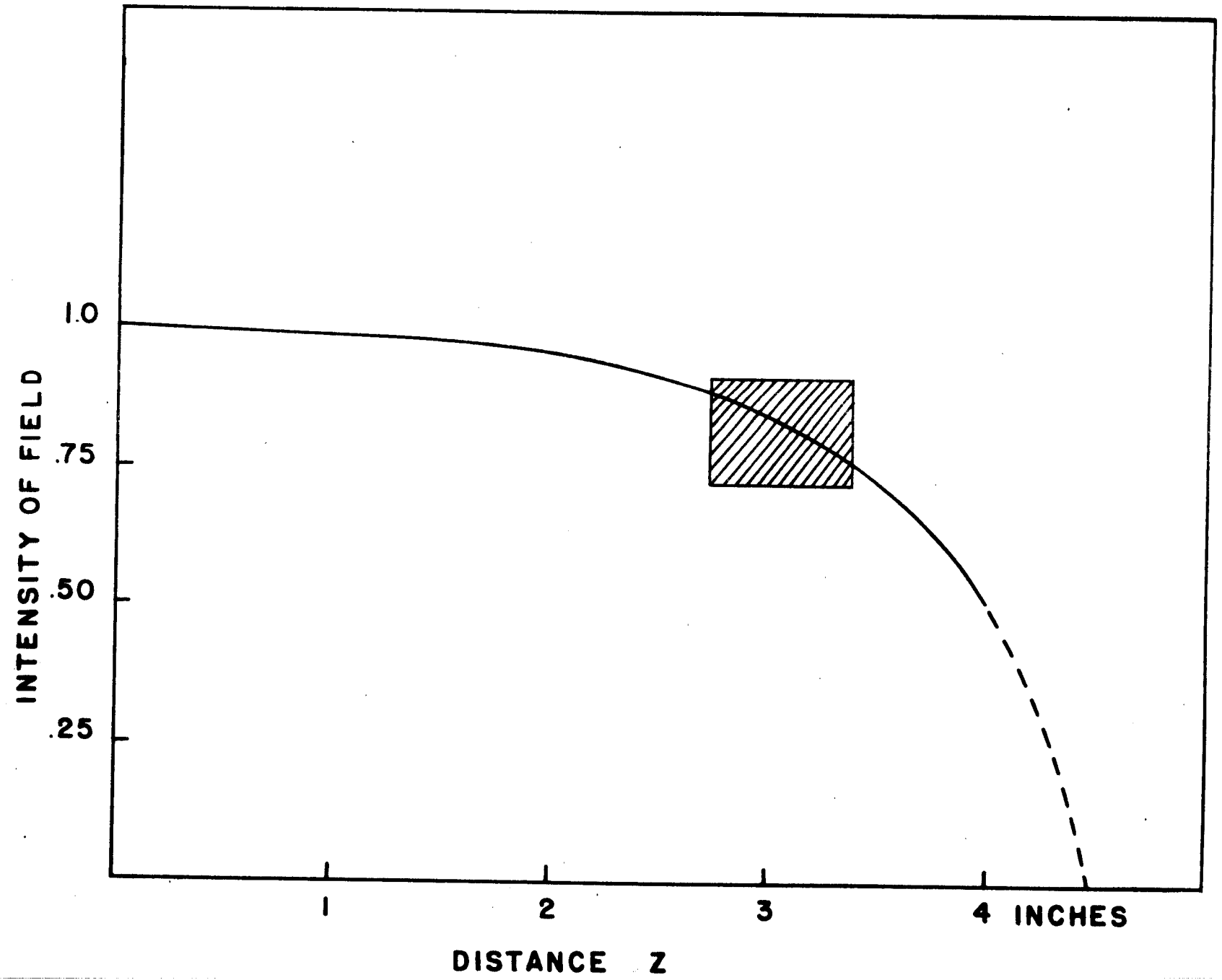
1.0
.75
.50
.25
INTENSITY OF FIELD
1
2
3
4 INCHES
DISTANCE Z

electron scatters from the detector at one end to the detector at the other end. It must then traverse the length of the solenoid in a time short compared to the integration time of the amplifier.

The first problem depends upon the size of the magnetic field and the dimensions of the detectors. The maximum radius needed as a function of the electron energy and the magnetic field has been calculated and is shown in Fig. 5. For the detectors used in this experiment, the spectrometer may be operated in the cross-hatched region. For the internal conversion lines of interest in Bi^{207} (not greater than about 1 MeV), no difficulty is expected since the fields used were greater than 25 kilogauss.

The second problem is more serious since it is obvious that some of the electrons will never have their full energy detected. To calculate the importance of this effect, the assumption is made that the particles are emitted isotropically initially from the source. Then the total number of particles emitted is proportional to the surface area of a sphere concentric with the source. This sphere is shown in Fig. 6 with the additional assumption that the source is a point source. This last assumption is a good one, since the total source intensity needed is only a few nanocuries which means that the total source area will be much smaller than that used for other types of spectrometers and, in our case, is usually less than 1 mm. Therefore, the number of particles emitted within an angle $\phi = 0$ to $\phi = \pi - \theta$ where θ is measured with respect to the axis of the solenoid, is proportional to fraction of the

Fig. 5. Maximum detector radius needed as a function of magnetic field and electron energy. The cross-hatched area corresponds to the detectors used.

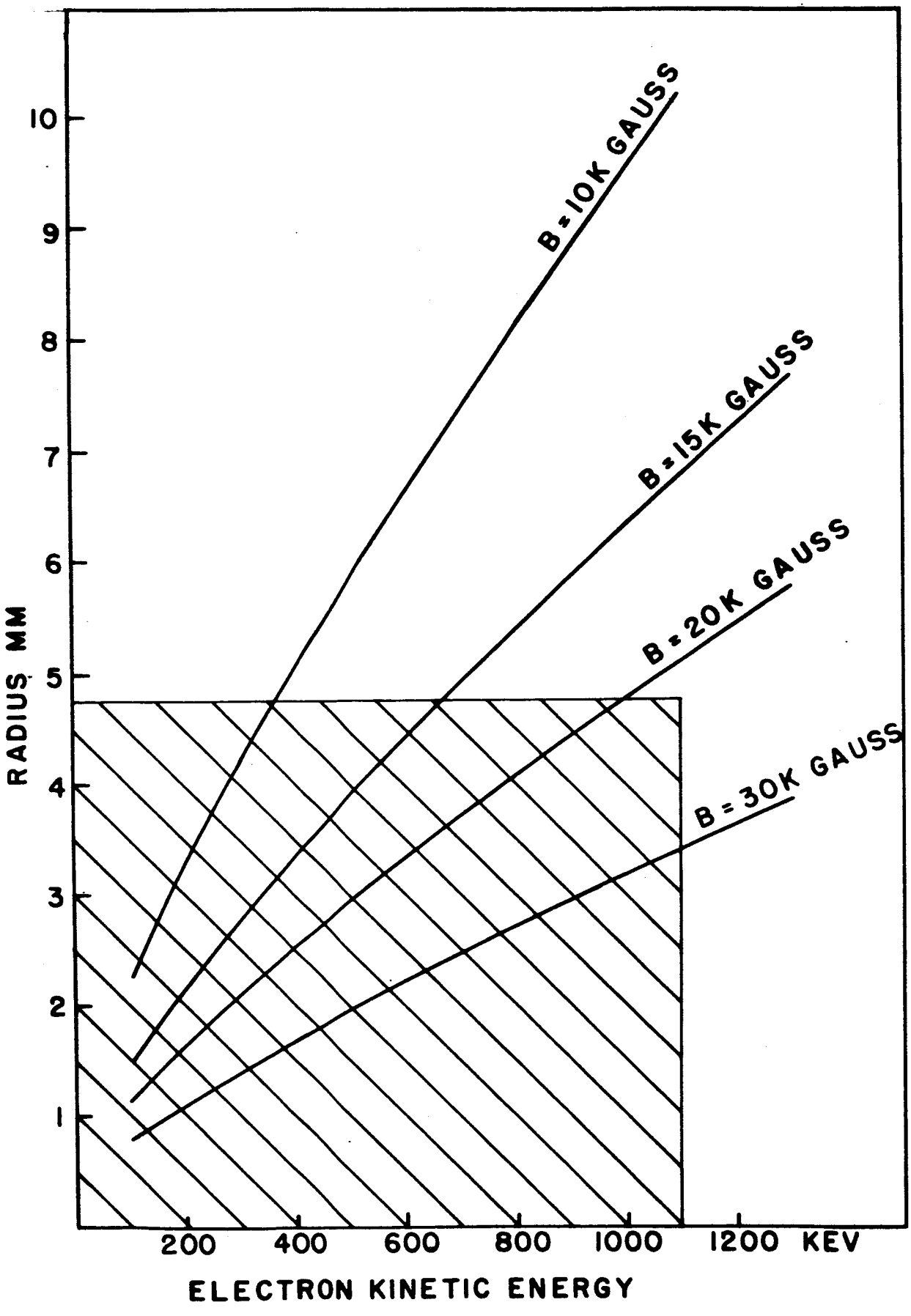
B = 10K GAUSS
B = 15K GAUSS
B = 20K GAUSS
B = 30K GAUSS
RADIUS MM
1
2
3
4
5
6
7
8
9
10
200
400
600
800
1000
1200 KEV
ELECTRON KINETIC ENERGY

Fig. 6. Sphere and angles used in calculating number of electrons collected in a specific time interval.

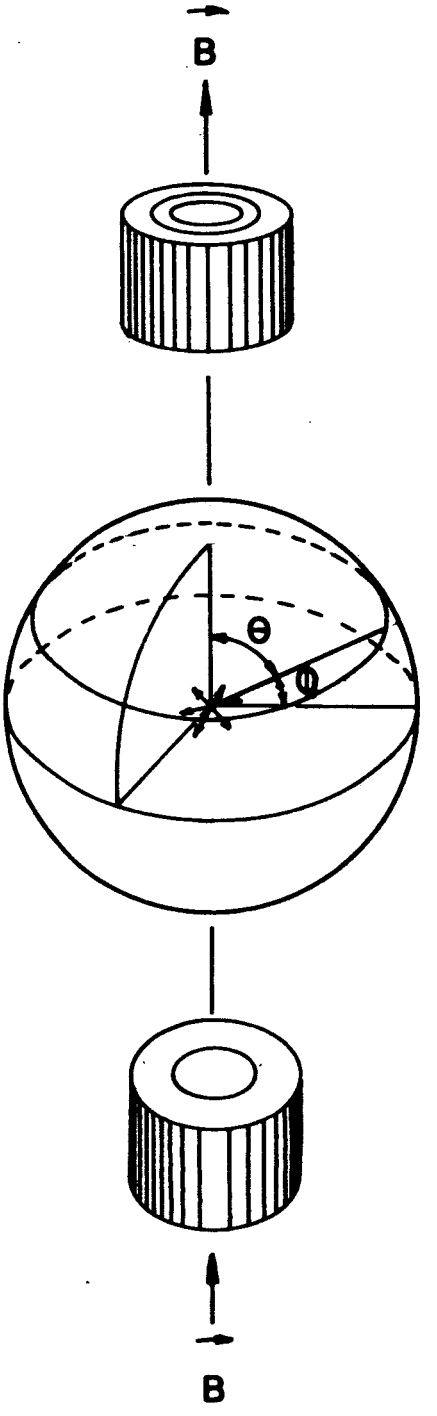
B
θ
φ
B

sphere swept out by rotating ϕ around the axis. Performing the integration, the number emitted with this angle is proportional to $\cos \theta$. The time of flight of the particles is determined by their component of velocity parallel to the field and by the distance from the source to the detectors. Solving the necessary equations, we find that the fraction emitted between $-\phi$ and $+\phi$ which have a time of flight too long to be collected is

$$N = \cos \theta = \left[\frac{mc^2}{t} \left(\left(1 - \left(\frac{z}{ct} \right)^2 \right)^{\frac{1}{2}} - 1 \right) \right]$$

where t is the collection time of the detecting system, in this case, the integration time of the amplifier. This fraction expressed as a percentage has been plotted as a function of integration time for electrons of different energies in Fig. 7. Only one traversal of the solenoid from source to detector has been plotted. However, even for several traversals, the fraction is quite small for integration times in the region of 1 microsecond. Therefore, this effect does not appear to make any substantial contribution to the data.

In any experiment where the effect under consideration is small, it is necessary to determine that the contribution from background radiation is not signigicant. The measured spectrum of the internal conversion lines of Bi^{207} taken with the spectrometer is shown in Fig. 8. The region from channel 160 has been expanded and is plotted in Fig. 9. Two additional sets of data are shown. A spectrum was measured with the superconducting magnet turned off and a background spectrum of nearly constant amplitude approximately 1% of the original spectrum

Fig. 7. This diagram plots the percentage of electrons whose velocity in the direction of the detectors is so small that complete charge collection will not be made if more than one traversal of the solenoid is required.

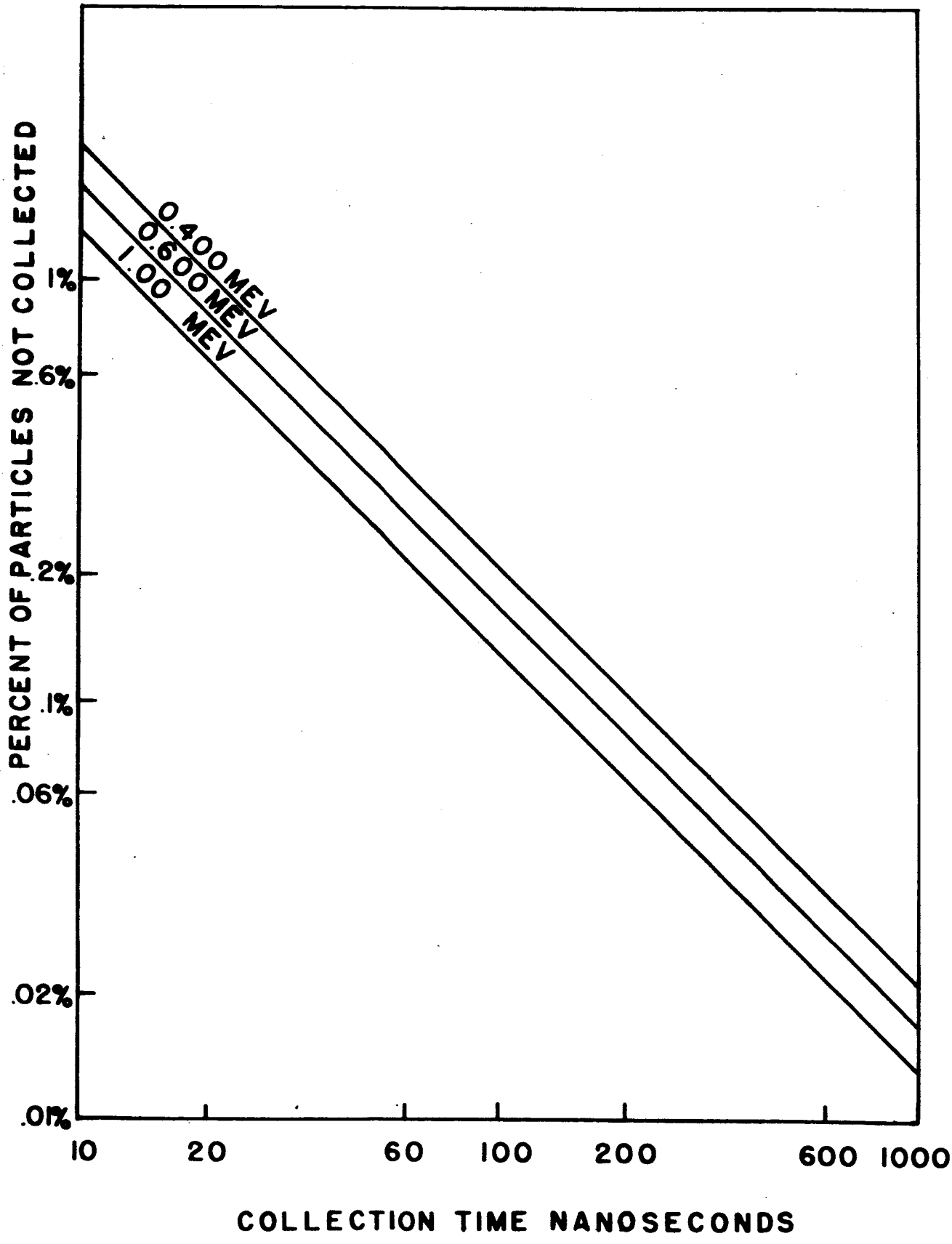
0.400 MEV
0.600 MEV
1.00 MEV
PERCENT OF PARTICLES NOT COLLECTED
1%
.6%
.2%
.1%
.06%
.02%
.01%
10
20
60
100
200
600
1000
COLLECTION TIME NANOSECONDS

Fig. 8. Measured spectrum of Bi^{207} obtained from superconducting magnet beta-ray spectrometer with both detectors operated in parallel, that is, with their outputs summed.

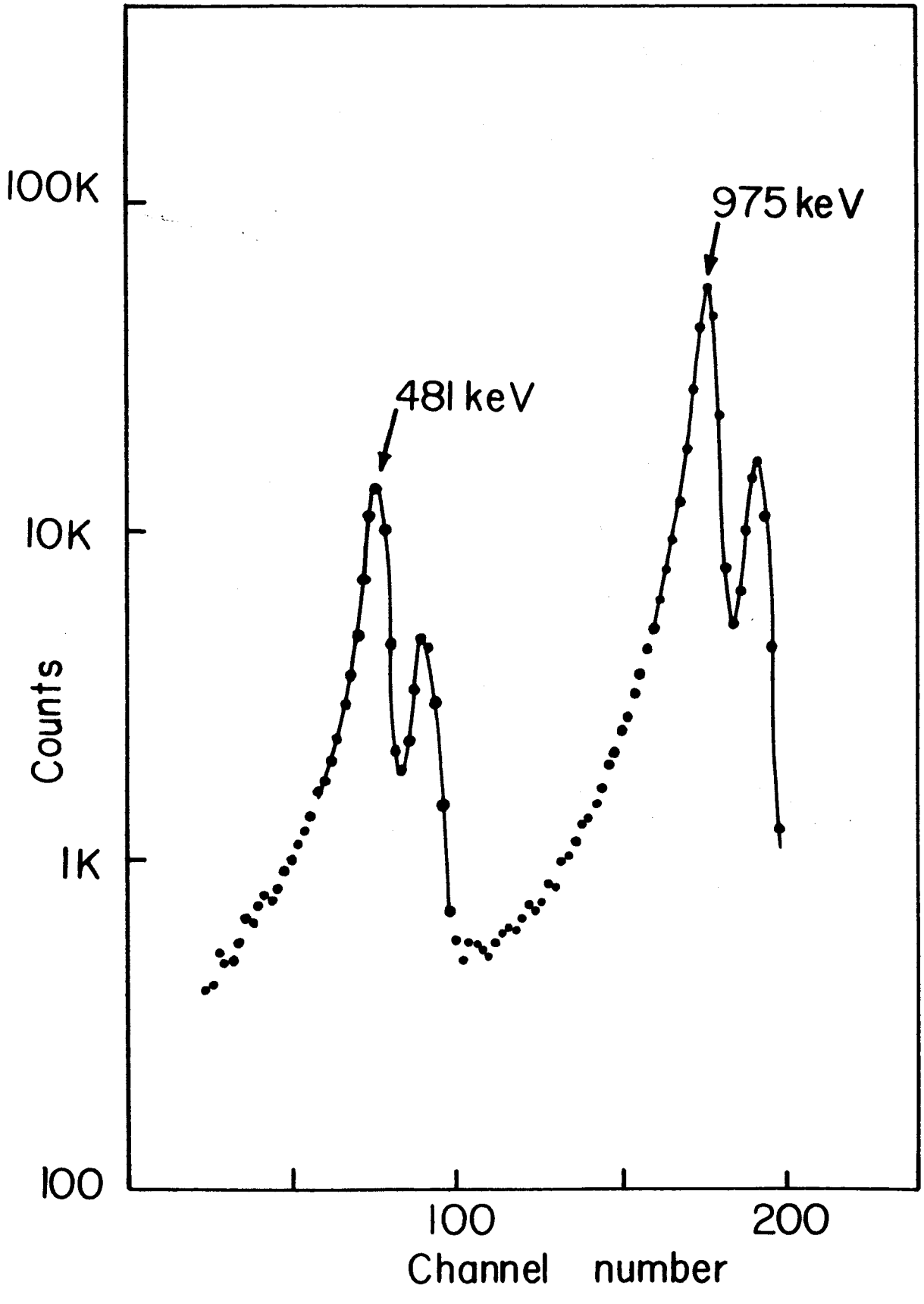
100K
10K
1K
100
Counts
481 keV
975 keV
100
200
Channel number

Fig. 9. Expanded portion of Fig. 8. Two background spectra are plotted one with no magnetic field and the other with no magnetic field and obsorbers in front of the detectors. The dashed line is the standard deviation of the spectrum obtained with the magnetic field turned on.

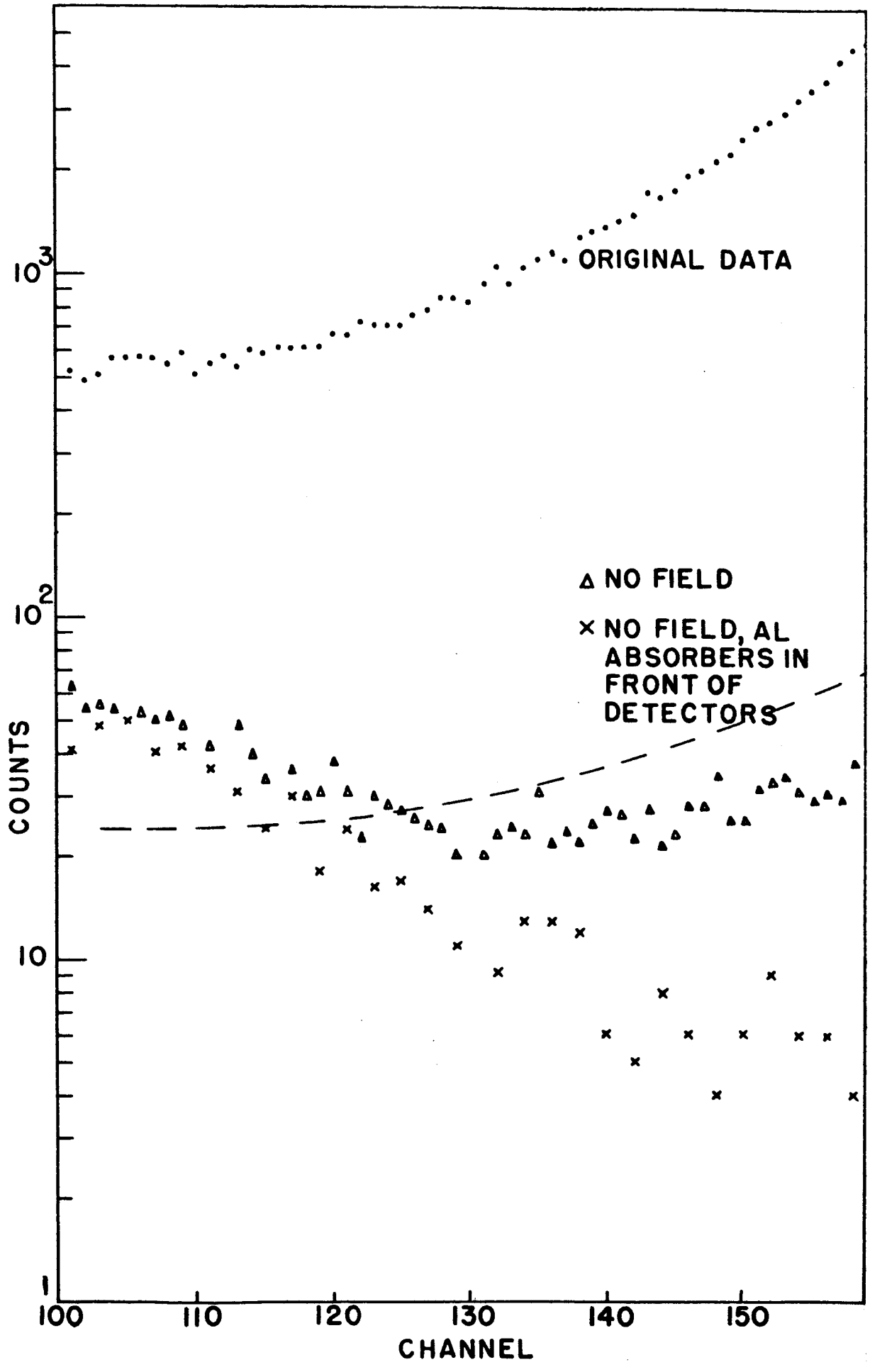
ORIGINAL DATA
Δ NO FIELD
× NO FIELD, AL ABSORBERS IN FRONT OF DETECTORS
COUNTS
CHANNEL
10^3
10^2
10
1
100
110
120
130
140
150

was observed. As a further check, aluminum absorbers were placed in front of the detectors to absorb the beta particles contributing to the above background spectrum. This is also shown in Fig. 9. This measurement determines the contribution of the gamma rays to the main spectrum. Both of these background contributions have been measured well below the peak of the internal conversion line and in the region where most of the contribution to the spectral distribution would be expected to be from the internal Compton effect. These measurements effectively rule out the possibility that the spectra was primarily background radiation.

One final check on the experimental data has not yet been performed. Although the source intensity is very low and the resulting source volume very small, the source mounting was on aluminized Mylar and there is some possibility that charge may have built up on the source after emission of electrons. This might distort the final electron distribution. A special source is now being made up for us by Nuclear Science and Engineering Corporation. This source will have a thin layer of aluminum flashed over it at the final stage of preparation in order to provide a conductive path for any charge.

Spruch and Goertzel[5] have performed a relatistic quantum mechanical calculation using the Born approximation for the simultaneous ejection of a K electron and the emission of a gamma ray in the case where the virtual radiation field is assumed to be magnetic in character. The 1063 keV transition in Bi^{207} is known to be M4 and we have calculated the theoretical electron distribution using this information and the results of Spruch and Goertzel. In comparing the theoretical

distribution with the experimental data, the resolution of the solid state detector must be taken into account. The internal conversion line was assumed to be symmetric about its peak and, since the internal Compton effect is present only on the low energy side, the high energy side was reflected about the peak channel to give a reasonable approximation to the undistorted conversion line. The theoretical contribution of the internal Compton effect can then be compared to the experimental data by simply folding the resolution of the detector into the theoretically calculated distribution. The intensity of the internal conversion line is also obtained by this procedure and is needed in the calculation of the amplitude of the theoretical distribution.

In the theoretical calculation of Spruch and Goertzel, the Born approximation was used, and the numbers are expected to be valid only for small atomic number and large transition energy. The requirement of small atomic number while not stringent is not satisfied for Bi^{207}, but the theoretical and experimental results are in good agreement as can be seen from Fig. 10.

Calculations using other theoretical results have been made both for the 975 keV conversion line and for the 481 keV conversion line.

Each of these theoretical calculations has a different basis which may or may not be expected to yield valid results for transitions from this nucleus and in this energy range.

Chang and Falkoff[6] assumed that the internal Comption effect could be described as the bremsstrahlung of the internal conversion electrons. As an electron in the K shell passes near the nucleus,

Fig. 10 Experimental data of the 975 keV internal conversion line of Bi^{207} compared with the following theoretical calculations

- Δ Spruch and Goertzel
- θ Baumann and Robl
- ● Chang and Falkoff
- ▲ Iakobson from formula depending on multipolarity of transition
- X Iakobson from multipolarity independent formula.

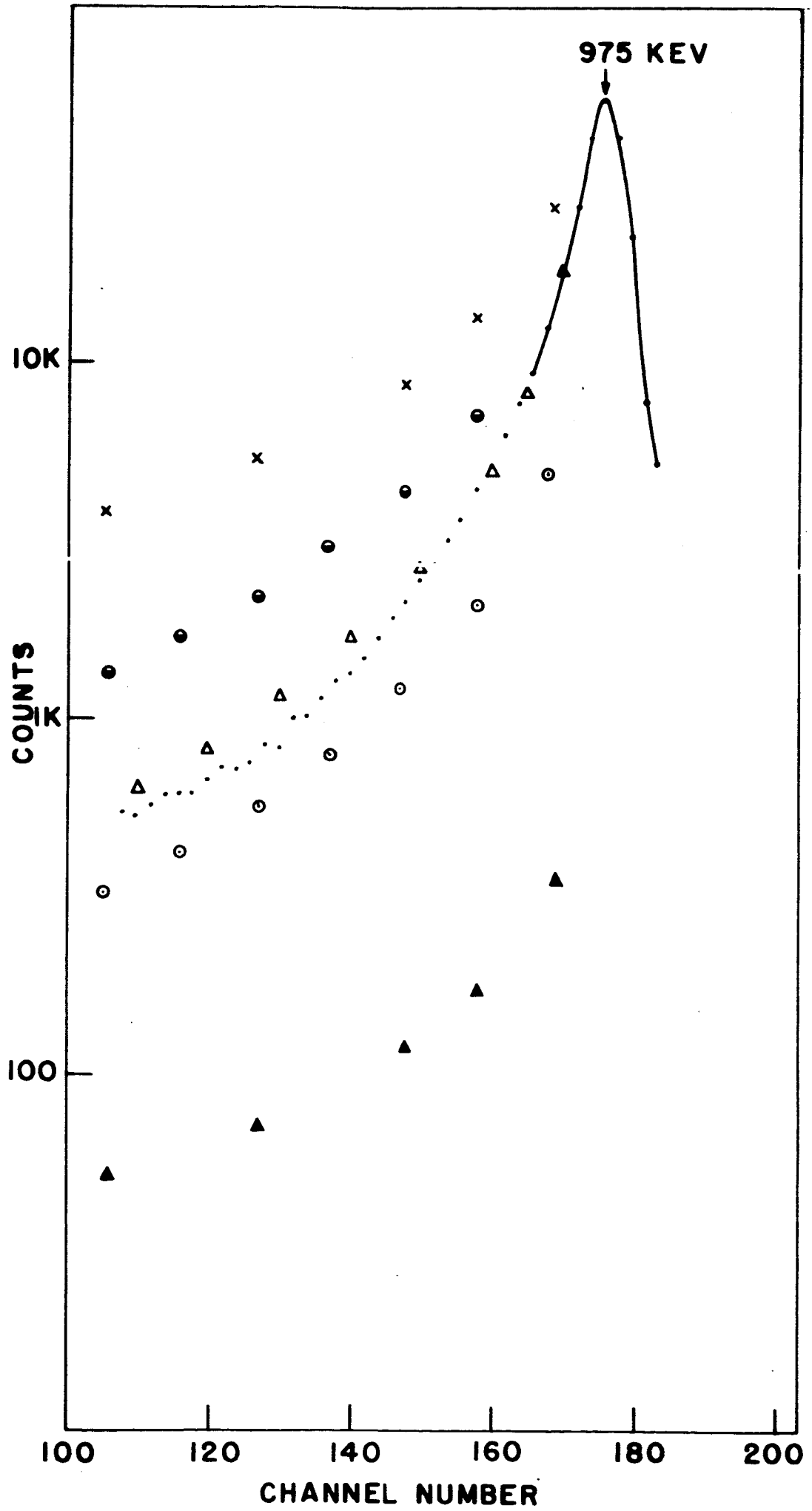
975 KEV
10K
1K
100
COUNTS
100
120
140
160
180
200
CHANNEL NUMBER

the transition energy may be given to it. It is then ejected from the shell, but in this process is given a large instantaneous acceleration which changes its velocity. Any radiation emitted during this change of velocity decreases the energy of the electron. This description is a semi-classical treatment and does not depend upon multipolarity; however, as can be seen from Figs. 10 and 11, the agreement with the experimental data is still relatively good.

This treatment has been extended by Baumann and Robl[7] in a quantum mechanical calculation which again considered only K shell electrons and low atomic number nuclei but taking into account the multipolarity of the transition. In detail, the calculation is somewhat more dependent upon the requirement of low atomic number than that of Spruch and Goertzel. In spite of this, the agreement with experiment is still very good.

The problem has also been treated by Iakobson[8] who adopted a non-relativistic perturbation theory approach with the requirement that the transition energy be much less than the electron rest energy. If his results are plotted as a comparison with the internal conversion coefficient, the dependence upon multipolarity disappears. In comparing this calculation with the experimental data, there is excellent agreement with the 481 keV transition data, but very poor agreement with the 975 keV transition data. The calculation is non-relativistic and the agreement with the lower transition is probably fortuitous.

In summary, the agreement of experiment and theory is a strong indication that the low energy distribution of the electrons is primarily that of the internal Compton effect. There are discrepancies in the shape

Fig. 11. Experimental data of the 481 keV internal conversion line of Bi^{207} compared with the following theoretical calculations

- Δ Spruch and Goertzel
- Θ Baumann and Robl
- ⊖ Chang and Falkoff
- ▲ Iakobson from formula depending on multipolarity of transition
- X Iakobson from multipolarity independent formula

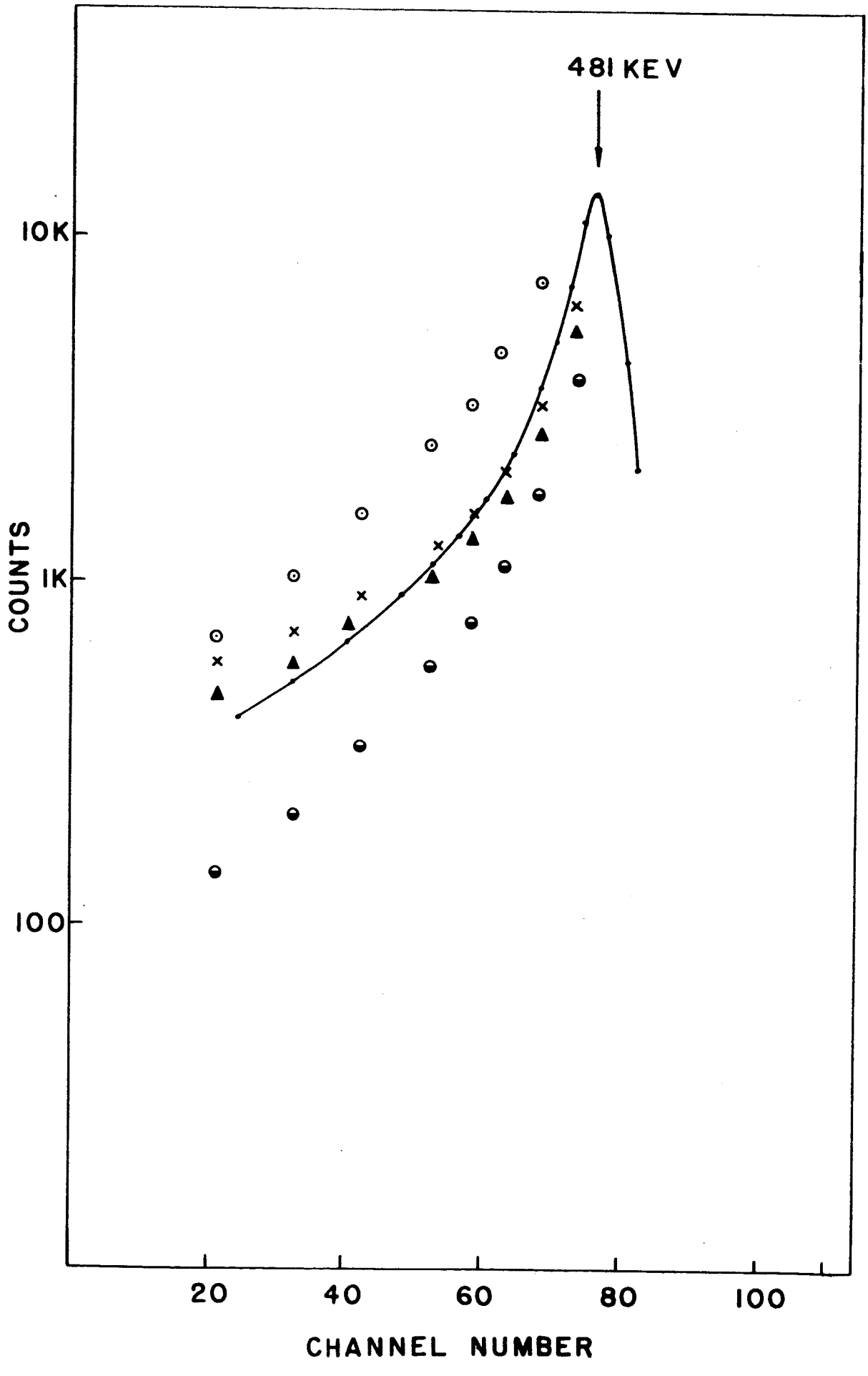
481 KEV
10K
1K
100
COUNTS
20
40
60
80
100
CHANNEL NUMBER

of the distribution reflecting the variety of approaches and approximations used in the theoretical calculations. More exact theoretical results are needed, therefore, before an adequate comparison of theory and experiment can be made.

(5) Ohmic contacts to silicon detectors.

The question of ohmic contacts to the silicon detector itself is a critical one for operation of the detector over a wide range of temperatures. As reported in the semi-annual status report for this grant year, contact to the lithium diffused side is made by using duPont Silver Cement between the stainless steel screw and the electroless gold plated surface. To date, this has given us the most reliable ohmic contact under varying ambient temperatures. However, the mechanical strenth of the contact is relatively poor. As a result, it has been necessary to bond the screw to the silicon wafer with Apiezon wax. At the temperature necessary to make the wax flow, the silver cement no longer adheres and occasionally the contact will break or become noisy.

The basic problem with such a contact is that it must be non-rectifying. Our experience with two different conducting epoxy cements indicate the difficulties that may arise. Each of these cements, Epoxy Products 3021 and Hysol K20, was easily applied and hardened at room temperature. Neither lost its adherence properties at temperatures well above the melting point of the Apiezon wax.

However, such an epoxy consists primarily of granules of silver which are in a colloidal suspension and are not involved in the hardening

process. Moreover, the actual cure times for the epoxy may be weeks. The effect of this was seen in the rectifying properties that developed in the Epoxy Products 3021 cement as a function of time. This rectification was probably a point contact effect with the silver granules. As the epoxy cured, the rectification became more pronounced. Moreover, the resolution of the detector during the one month period of observation was degraded by a factor of two, and the internal conversion line peaks developed an asymmetry on the low energy side.

On the other hand, the Hysol K20 has not developed such a diode characteristic even after three months leading us to the hope that this contact may prove more reliable. However, it will be necessary to investigate the conduction characteristic as a function of temperature in order to establish that the contact remains ohmic over a wide range, since the epoxy and silver may have very different coefficients of expansion.

The contact to the gold surface barrier layer has usually been made by bonding a gold wire with General Cement silver print to a drop of Aquadag on the surface. This contact is not stable against moisture and is very delicate. Also, it has been suggested[9] that a true surface barrier is not formed at this surface. Rather, an oxide layer whose thickness depends on the speed of the final etch may be formed. If this is the case, it should be feasible to make a more reliable pressure contact to this surface. The results of this will be reported later.

(6) Studies of high Z semiconductors for radiation detectors.

An intensive program for the development of solid state radiation detectors from single crystals of silicon and germanium has been in progress in laboratories throughout the country. The effectiveness of these devices for charged particles has stimulated a need for counters made from high Z materials which will be efficient, at least more efficient than germanium, for detection of gamma rays.

Since very little work has been done in this area, use of the literature is limited to the systematic application of relevant experimental data compiled from work with compound semiconductors, as well as theoretical research which has been done on the nature of the elements as they appear in the periodic table. For example, one of the first parameters to be considered in the evaluation of a substance to determine its suitability for radiation detection is the energy of the band gap, E_g , with optimum values being near that of silicon (1.4 eV). In general, the lower the band gap, the less suitable is the material for radiation detectors since it requires less thermal energy to excite electrons into the conduction band. As a result, for low energy gaps, the intrinsic carrier concentration may be much higher than that produced by any dopant. Hence lithium ion compensation will then be impossible.

In addition to a suitable band gap, one must also have reasonable lifetimes and mobilities of the charge carriers to insure nearly complete charge collection in any potential radiation detection material.

The very high Z of lead sulfide makes this compound an attradtive substance for consideration as a radiation detector. Actual experience

showed, however, that the cubic lattice of this material produced weak crystalline bonds which were unable to withstand the lapping and sanding procedures necessary in the fabrication of radiation detectors. Even with the most delicate handling, cleavage of the crystal was too common.

This experience with lead sulfide indicated a need for further consideration of crystal structure and bonding in semiconductors. Since both silicon and germanium are relatively easy to process, it was decided to explore materials of similar structure. In 1950 Garyunova[10] concluded that III-V compounds which have a zinc-blende structure, have chemical bonds between atoms which are predominantly covalent and nearly identical to the bonding found in elements of Group IVb elements. Subsequent experimentation showed that these compounds are structural analogs of the IVb atoms and are indeed semiconductors in every sense. Since that time, numerous papers have been published on the preparation and properties of III-V compound semiconductors. For this reason we have begun our efforts in this area with the III-V compounds.

The band structure of these compounds is closely related to the nature of the chemical bonding of the lattice. In deducing the electrical properties, it is helpful to compare the lattice and bonding properties of the Group IV elements which are well understood with those of the III-V compounds. Group IV atoms are bonded in a diamond lattice, each atom having four nearest neighbors in a tetrahedral structure. The lattice of III-V compounds is identical to that of the Group IV elements with the exception that, while the diamond lattice of Group IV is populated with atoms of only one type, this zinc-blende lattice is occupied alternately by both A and B atoms. One interesting

characteristic of this is that the behavior of the charge carriers in the zinc-blende structure is more related to the structure of the sublattices than to the lattice as a whole. Therefore, the band structure of III-V compounds is simpler than that of the Group IV elements since the diamond lattice has eight atoms/unit cell giving it a relatively complicated symmetry, while a III-V sublattice has only four atoms/unit cell.

This difference in symmetry is responsible for the higher mobilities of charge carriers and the shorter lifetimes in III-V compounds relative to the Group IV elements. However, the mobilities and energy gaps are also related to the effective ionicity of the chemical bond. The greater the effective ionicity between the atoms of a crystal, the greater is the probability of ion scattering and the lower will be the mobilities of the charge carriers. This effective ionicity between two component ions of a III-V compound is a function of the polarization of the chemical bond between the atoms. In order to see this, it is necessary to consider in some detail the type of bonding that occurs in III-V compounds.

The bonding of atoms in the Group IV elements is purely covalent in rature, but III-V compounds have a combined covalent and ionic bond formation. In ionic bonding, the cation is relatively small and the electrons are tightly bound, since the absence of electrons from the valence band gives a positive charge to the nucleus which attracts the remaining electrons. On the other hand the excess of electrons in the anion results in a smaller electrostatic attraction for the electrons and, as a result, the anion is rather large and easily deformed.

These negative charges on the anion are attracted to the positively charged cation, reducing the effective negative and positive charge on the anion and cation. Such an effect is termed polarization of the anion. Generally, the polarization increases with an increase in the charges on the ions and with decreasing cation size.

The formation of this type of ionic bond does not usually result in a pure ionic state. Rather, the polarization of the anion causes the covalent characteristic of the bonding, since there is a high electron density between the lattice sites causing the formation of spin-saturated electron pairs. This is essentially the same effect as a covalent bond. This bond is therefore weaker than a pure ionic bond in terms of producing a lower energy gap and a higher mobility for the charge carriers. There is a dependence of the energy gap on the ratio of the sizes of the cation and anion, the mean main quantum number, and the difference in the electronegativity of the component ions. It is possible to estimate the band gap on the basis of these three quantities in order to determine their possible use as radiation detectors.

Single crystals of III-V compounds which have a [111] orientation are structured in alternate layers of Group III and Group V atoms. If a wafer is obtained from an ingot by slicing normal to this axis, one face of the crystal will have a surface layer of Group III atoms, while the other face will have a surface layer of Group V atoms. Since only a minimum of energy is required to break the bonds between the planes, it is improbable that the break will occur in any other manner. Conventionally, the Group III side of such a crystal is termed the A side or [111] side, while the Group V side is the B side or the [111] surface. The actual

identification of these sides is relatively simple, since the B surface is more chemically reactive than the A side. Consequently, a polish etch composed of 3 parts of a 6:2:1 mixture of HNO_3, HF, and fuming HNO_3 and of 2 parts H_2O, when cooled to approximately 0°C has been found by us to etch the B side of the crystal, but has little apparent reaction on the A side. Such an etching technique is also very useful in the gross identification of twinning, grain boundaries, and polycrystalline materials. Determination of the sides is of extreme importance, since it was discovered by Gatos[11] that crystals grown from the A surface of a seed of a III-V compound will result in twinning and grain boundaries. On the other hand, if the crystals are grown from the B surface, all other factors being equal, single crystals of relatively low dislocation densities will result.

Moreover, Minamoto[12] has found that p-n junctions prepared on the A surface typically showed low breakdown voltages and high reverse currents. However, "B junctions" showed a relatively high breakdown voltage and reverse currents that were an order of magnitude lower than those of "A junctions."

Crystals of high purity zinc doped, p-type gallium antimonide with a [111] orientation were obtained from Semi-Elements. Although found to be polycrystalline when etched with the 6:2:1:2 H_2O etch. An X-ray diffraction picture also served to support the conclusions drawn from the appearance of the etch. Unfortunately, this etch was not perfected until several crystals had been processed. Despite this, a number of technical experiments were carried out to determine chemical

and physical processing techniques. In general, the crystals were quite similar to germanium with regard to these techniques.

The primary difficulty was encountered when an attempt was made to form a p-n junction by diffusion of lithium. Although an apparent lithium alloy surface was actually obtained by applying a lithium-in-oil suspension to the top surface and diffusing for five minutes at 600°C, the conductivity of this surface, as measured by a hot and cold probe operated at room and liquid nitrogen temperature, remained p-type. Since lithium should be a donor in gallium antimonide, such an obviously alloyed surface should be n-type. The conclusion was reached that the lithium had precipitated out of the gallium antimonide at a very rapid rate. This same type of precipitation occurs in germanium and silicon although at a much reduced rate.

At this point, a slightly different technique was adopted. The problem of diffusion of impurities into single crystals can be viewed from the standpoint of the formation of a solid solution. Vacant sites into which impurity atoms or ions may enter must be available for either diffusion or solution to take place. The concentration of these vacancies as well as the energy with which the impurity particles are bound to the solvent or lattice, are the controlling factors in the rate which these processes take place.

There are three different types of solid solutions to be considered: 1) substitutional, 2) interstitial, and 3) defect.

In a substitutional type solid solution, the structure of the solvent remains unchanged. The impurity atom enters a vacant site in the lattice and becomes an integral part of the lattice structure, evidenced

only by a change in the electrical properties of the crystal in cases where the impurity atom has a different number of bonding electrons than do its nearest neighbors in the lattice.

The probability of an impurity atom entering a lattice substitutionally is increased with the following conditions:

1) Solute and solvent must have comparable atomic dimensions (less than 14% difference).
2) Similar crystal structure.
3) Similar outer electron shells.
4) A small difference in electronegativity.

In our laboratory tellurium has been successfully diffused into p-type GaSb crystals and a p-n junction formed. The following data would indicate that the tellurium should enter the lattice substitutionally at antimony vacancy sites in preference to gallium vacancy sites.

Atom	Atomic Radius	Structure	Valence Shells	Electro-negativity
Ga	1.41 Å	orthorhombic	Ar $3d^{10}4s^{2}4p^{1}$	1.6
Sb	1.59 Å	rhombohedral	Kr $4d^{10}5s^{2}5p^{3}$	1.9
Te	1.60 Å	hexagonal	Kr $4d^{10}5s^{2}5p^{4}$	2.1

The published diffusion constant of tellurium in GaSb is also of interest at this point, since it was experimentally determined in our laboratory that a measureable diffusion was not obtained at temperatures below 650°C.

As can be seen by the following data, the diffusion constant has a sharp increase at this temperature.

DIFFUSION CONSTANTS OF Te IN GALLIUM ANTIMONIDE

D_{400}	0.06 cm^2/sec
D_{450}	0.47
D_{550}	1.20
D_{650}	42.00

Interstitial solid solutions usually involve impurity atoms of small radii, such as lithium, boron, hydrogen, nitrogen, carbon, and oxygen. The formation of an interstitial solid solution in a semiconductor is necessary when ion-drift compensation is used to produce a wide depletion region. Such a drift would be impossible with a substitutional impurity, since these atoms are tightly bound to the lattice, while an interstitially diffused atom is free to move throughout the crystal as an ion under the influence of an electric field at an elevated temperature.

When lithium is diffused into a germanium or silicon crystal, a very dense surface alloy is formed and the lithium may be drifted through the crystal under a reverse bias with this reservoir of ions as a source of supply. The alloy region must have a sufficiently high lithium concentration to form a sharp p-n junction in the crystal so that the necessary diode can be formed for drifting purposes.

As noted before, the lithium precipitation rate was very rapid and no junction could be maintained using only lithium as an n-type layer.

References

1. M. E. Rose, Phys. Rev. 53, 715 (1938).
2. Tenth Scintillation and Semiconductor Counter Symposium, March, 1966, papers by T. V. Blalock, K. F. Smith and J. E. Cline, and V. Radeka and R. L. Chase.
3. T. V. Blalock, Tenth Scintillation and Semiconductor Counter Symposium, March, 1966 (to be published).
4. M. M. El-Shishini and W. Zobel, Tenth Scintillation and Semiconductor Counter Symposium, March, 1966 (to be published).
5. Larry Spruch and G. Goertzel, Phys. Rev. 94, 1671 (1954).
6. C. S. W. Chang and D. L. Falkoff, Phys. Rev. 76, 365 (1949).
7. K. Baumann and H. Robl, Z. Naturforschg. 9a, 511 (1954).
8. A. M. Iakobson, JETP, 29, 703 (1955).
9. F. S. Goulding, UCRL-16231 (unpublished).
10. N. A. Goryunova and A. P. Obuchov, Zhur. Tekh, Fiz. 21, 237 (1951).
11. H. C. Gatos and M. C. Lavine, J. Appl. Phys. 31, 212 (1960).
12. M. T. Minamoto, J. Appl. Phys. 33, 1826 (1962).
13. H. Reiss, C. S. Fuller, and F. J. Morin, Bell Syst. Tech. Jour. 35, 535 (1956).

Fig. 12. Identification of polycrystalline gallium antimonide, as evidenced by the 6:2:1:2 H_2O etch at 0°C.

However, Reiss, Fuller and Morin[13] have shown that the formation of a p-n junction on germanium and silicon will prevent the precipitation of lithium from the region enclosed by this junction. However, the junction must have a heavily doped n-type layer so that the potential barrier will prevent the lithium ions from diffusing to the surface where they can combine with the surface oxide layer and precipitate out. With this in mind, tellurium was diffused into the gallium antimonide. Then lithium was diffused into the crystal, passing easily through the tellurium layer. Probing techniques indicated that the lithium did in fact remain in the crystal without precipitating when a p-n junction had previously been formed with tellurium. It has not as yet been possible to attempt drifting lithium through such a crystal since the commercial supplier has so far only given us polycrystalline material. However, as high purity materials become available in single crystal form, it should be possible to apply this technique to gallium antimonide and attempt lithium-ion compensation.

The third type of solid solution is termed defect, and is usually a stoichiometric effect caused by an excess of one of the constituent elements of the compound. This effect results in an electrical imbalance in the crystal. Such a solution is not appropriate for radiation detectors, since the crystal lattice usually has a preponderance of vacancies which interfere with the homogeneous distribution of impurity ions.